Electronic Structure of Bispentalene Complexes of Titanium, Zirconium, and Hafnium: A Photoelectron Spectroscopic Study

Rolf Gleiter,*[,†] Sabine Bethke,[†] Jun Okubo,[†,§] and Klaus Jonas[‡]

Organisch-Chemisches Institut der Universität Heidelberg, Im Neuenheimer Feld 270, D-69120 Heidelberg, Germany, and Max-Planck-Institut für Kohlenforschung, Kaiser-Wilhelm-Platz 1, D-45470 Mülheim an der Ruhr, Germany

Received March 26, 2001

The geometrical parameters of the bis(pentalene) complexes of titanium, zirconium, and hafnium (**3a**−**c**) have been calculated by applying the RHF method. For **3a** a structure with C_1 symmetry results, whereas for **3b**,**c** D_2 symmetry is predicted. The torsional angles between the two pentalene ligands are calculated to be 56° (**3a**), 51° (**3b**), and 50° (**3c**). The orbital sequence of the six highest occupied molecular orbitals agrees very well with the ionization energies measured by PE spectroscopy of **3a**−**c**. These measurements support a structure with D_2 or closely related symmetry.

Introduction

Complexes with cyclopentadienyl ligands are legion and very well established in transition metal and main group metal chemistry. Much less studied are complexes with coordinated pentalene, having a bicyclic structure with two fused five-membered carbocycles. Among the first pentalene complexes reported were compounds with two transition metal nuclei such as the dinickel and dicobalt compounds **1a** and **1b**.[1] Recently Jonas et al.[2a−c] as well as Cloke et al.[3,4] reported some complexes with one or two pentalene ligands coordinated to a single metal center. Jonas et al. succeeded in synthesizing complexes with the parent pentalene such as **2** and **3**,[2b] whereas Cloke et al. were successful in preparing

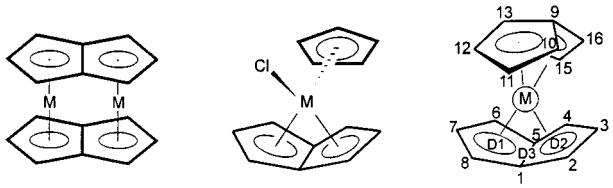

M = Ni, Co **1a 1b** | M = Ti, Zr **2a 2b** | M = Ti, Zr, Hf **3a 3b 3c**

compounds with R_3Si-substituted pentalene ligands, i.e., $Ta\{\eta^8\text{-}C_8H_4(1,5\text{-}SiMe_3)_2\}Cl_3$[3] and $M\{\eta^8\text{-}C_8H_4(1,4\text{-}Si^iPr_3)_2\}_2$ (M = Th, U).[4] X-ray studies of single crystals of the thorium complex reveal the presence of two isomers in the solid state, one with near S_4 symmetry and one with D_2 symmetry.[4a] The mononuclear pentalene complexes comprise a new type of bonding of the pentalene ligand.[2a,5,6] Thus, the complexes justify a detailed investigation of their electronic structure. Such studies on the thorium and uranium compounds have been published recently.[4b] In this paper we report the He(I) and He(II) photoelectron (PE) spectra of **3a**−**c** together with ab initio calculations in order to study the orbital energies and the structural parameters of the complexes.

Results

Structures of 3a−c. Experimental values for the geometrical parameters of **3a**−**c** are not available, but these compounds and the closely related bis(2-methylpentalene) complexes have been studied in detail by NMR spectroscopy. Selected NMR data for Ti(2-methylpentalene)$_2$ have been published as a preliminary report.[2b]

The ^1H and ^{13}C NMR spectra of the bispentalene complexes and their dimethyl derivatives are temperature dependent. The spectra of **3a** measured at −80 °C are consistent with its having D_2 symmetry. In general, the NMR spectra of these complexes indicate that the torsional angle between the pentalene ligands is neither 0 nor 90°, but somewhere in between. At higher temperature a libration of the pentalene ligands occurs (see ref 2b). The barrier of this process is higher for the titanium complexes than for the corresponding zirconium and hafnium compounds.[2d]

† Heidelberg.
‡ Mülheim.
§ Present address: Dept. of Chemistry, Tokyo Denki University, Tokyo.

(1) Katz, T. J.; Rosenberger, M. *J. Am. Chem. Soc.* **1963**, *85*, 2030−2031. Katz, T. J.; Acton, N. *J. Am. Chem. Soc.* **1972**, *94*, 3281−3283. Katz, T. J.; Acton, N.; McGinnis, J. *J. Am. Chem. Soc.* **1972**, *94*, 6205−6206.

(2) (a) Jonas, K.; Gabor, B.; Mynott, R.; Angermund, K.; Heinemann, O.; Krüger, C. *Angew. Chem.* **1997**, *109*, 1790−1793; *Angew. Chem., Int. Ed. Engl.* **1997**, *36*, 1712−1714. (b) Jonas, K.; Kolb, P.; Kollbach, G.; Gabor, B.; Mynott, R.; Angermund, K.; Heinemann, O.; Krüger, C. *Angew. Chem.* **1997**, *109*, 1793−1796; *Angew. Chem., Int. Ed. Engl.* **1997**, *36*, 1714−1718. (c) Gabor, B.; Jonas, K.; Mynott, R. *Inorg. Chim. Acta* **1998**, *270*, 555−558. (d) Jonas, K.; Mynott, R.; Gabor, B.; Kolb, P.; Kollbach, G.; Rufinska, A. To be published.

(3) Abbasali, Q. A.; Cloke, F. G. N.; Hitchcock, P. B.; Joseph, S. C. P. *J. Chem. Soc., Chem. Commun.* **1997**, 1541−1542.

(4) (a) Cloke, F. G. N.; Hitchcock, P. B. *J. Am. Chem. Soc.* **1997**, *119*, 7899−7900. (b) Cloke, F. G. N.; Green, J. C.; Jardine, C. N. *Organometallics* **1999**, *18*, 1080−1086.

(5) Butenschön, H. *Angew. Chem.* **1997**, *109*, 1771−1773; *Angew. Chem., Int. Ed. Engl.* **1997**, *36*, 1695−1697.

(6) Costuas, K.; Saillard, J.-Y. *J. Chem. Soc., Chem Commun.* **1998**, 2047−2048.

10.1021/om0102403 CCC: $20.00
Publication on Web 09/07/2001

Table 1. Relative Energies for M = Ti, Zr, Hf (3a−c)[a]

M	D_{2h}	D_2	D_{2d}	C_1
Ti	39.9	2.2	15.3	0.0
Zr	28.5	0.0	8.0	
Hf	28.3	0.0	7.6	

[a] All values in kcal/mol.

DFT ab initio calculations on **3a** suggest D_{2d} symmetry.[6] To obtain the energies of the highest occupied molecular orbitals, we have carried out quantum chemical calculations on **3a**−**c**, using the RHF method and the LANL2DZ basis set[7] including pseudopotentials, and relativistic corrections[8] were applied. The calculations were carried out with the Gaussian 94 program.[9] Especially for late transition metal complexes the RHF method could have difficulties due to insufficient inclusion of electron correlation. However, calculations on the structurally related compounds CpMCl(η^8-C_8H_6) with M = Ti (**2a**) and M = Zr (**2b**) reproduced the geometrical parameters obtained by X-ray investigations[2b] with high accuracy.[10] The minimization of all geometrical parameters of **3a**−**c** as well as the free pentalene ligands yielded the relative energies of Table 1.

For **3b** and **3c** the calculations predict D_2 symmetry of the mononuclear complexes. The torsional angles θ between the C1−C5 and C9−C13 bonds were calculated to be 51° (**3b**) and 50° (**3c**). In the case of **3a** our calculations predict that the global minimum has C_1 symmetry. The torsional angle θ was calculated to be 56°. The C_1 minimum is only 2.2 kcal/mol lower than the energy predicted for the structurally related conformation having D_2 symmetry. The most important distances and angles calculated for **3a**−**c** are summarized in Table 2. The calculated bond lengths in the pentalene skeleton of **3a**−**c** differ only slightly. The variation is largest in **3a** (1.39−1.45 Å) and smallest in **3b** and **3c** (1.40−1.45 Å). In all three cases the pentalene ligands deviate from planarity. The angle D1−D3−D2 (see formulas) is calculated to be 152° for **3b** and 151° for **3c**. In the case of **3a** one pentalene ligand is found to be bent by 157°, the other by 149°. Due to this bending the overlap between the metal and ligand orbitals is enhanced.

In view of our spectroscopic investigations discussed below, the sequence of the six highest occupied molecular orbitals as a function of the torsional angle θ was of some interest. As an example we show in Figure 1 a correlation diagram of the six highest occupied MOs of

Table 2. Most Relevant Distances and Angles Calculated for 3a−c[a]

	3a (C_1)	**3b** (D_2)	**3c** (D_2)
M−C1	2.15	2.34	2.32
M−C5	2.19	2.34	2.32
M−C2	2.35	2.56	2.59
M−C4	2.41	2.60	2.52
M−C6	2.55	2.56	2.59
M−C3	2.54	2.75	2.73
M−C7	2.68	2.75	2.73
M−C8	2.35	2.60	2.52
C1−C2	1.45	1.44	1.45
C1−C8	1.44	1.45	1.45
C3−C4	1.42	1.41	1.44
C6−C7	1.39	1.43	1.40
C1−C5	1.45	1.45	1.44
D1−M−D2[b]	55.97	51.37	52.01
θ[c]	55.56	50.60	49.29
D1−D3−D2[b]	149.46	152.28	151.11
D3−M−D3′[b]	166.79	180.00	180.00

[a] The distances are given in Å, the angles in deg. The results were derived with the LANL2DZ basis. [b] For the definition see formula. [c] C1 C5 C9 C13 (see also Figure 1).

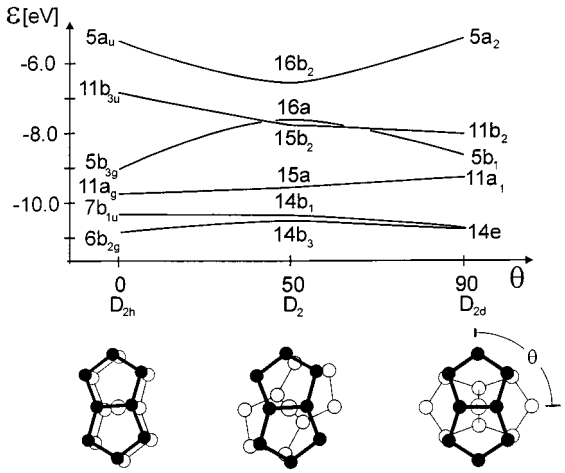

Figure 1. Correlation diagram of the six highest occupied molecular orbitals of **3a** as a function of the torsional angle θ. The energies were derived with the LANL2DZ basis.

3a as a function of θ. It should be noted that the correlation diagrams for **3b** and **3c** look very similar. From Figure 1 it follows that the highest occupied MO (HOMO) shows a minimum at $\theta = 50°$ (D_2 point group), whereas $5b_{3g}$ shows a maximum at the same value of θ. In contrast to these two MOs, the 11 b_{3u} orbital is stabilized when going from point group D_{2h} to D_{2d}. The remaining three D_{2h} MOs ($11a_g$, $7b_{1u}$, $6b_{2g}$) correlate smoothly with their D_{2d} counterparts, $11a_1$ and 14e. As a result of the changes just described, for point group D_2 two groups of equally spaced MOs result which are separated by quite a substantial gap between the third and the fourth MO shown in Figure 1.

To elaborate the reasons for the change in energy of the $5a_u$, $11b_{3u}$, and $5b_{3g}$ MOs as a function of θ, we consider the corresponding wave functions. To support our qualitative arguments, we use—in addition to symmetry criteria—the results of a Mulliken population analysis for **3a** in the point groups D_{2h}, D_2, and D_{2d}. The metal character of the wave function is given in Table 3 (see below). In Figure 2 we have shown the four linear combinations which result from the ligand orbitals π_5 and π_4. The HOMO can be described as the antibonding linear combination of the π_5-pentalene orbitals. For

(7) Hay, P. J.; Wadt, W. R. *J. Chem. Phys.* **1985**, *82*, 270−283.
(8) Dunning, T. H.; Hay, P. J. *Modern Theoretical Chemistry*; Plenum Press: New York, 1977; Vol. 3.1.
(9) Frisch, M. J.; Trucks, G. W.; Schlegel, H. B.; Gill, P. M. W.; Johnson, B. G.; Robb, M. A.; Cheeseman, J. R.; Keith, T.; Petersson, G. A.; Montgomery, J. A.; Raghavachari, K.; Al-Laham, M. A.; Zakrzewski, V. G.; Ortiz, J. V.; Foresman, J. B.; Cioslowski, J.; Stefanov, B. B.; Nanayakkara, A.; Challacombe, M.; Peng, C. Y.; Ayala, P. Y.; Chen, W.; Wong, M. W.; Andres, J. L.; Replogle, E. S.; Gomperts, R.; Martin, R. L.; Fox, D. J.; Binkley, J. S.; Defrees, D. J.; Baker, J.; Stewart, J. P.; Head-Gordon, M.; Gonzalez, C.; Pople, J. A. *Gaussian 94*; Gaussian, Inc.: Pittsburgh, PA, 1995.
(10) RHF/6-311G* calculations for **2a** compared to geometrical parameters obtained by X-ray investigations[2b] yielded deviations in Ti−C bond lengths between 0.05 and 0.00 Å, deviations of C−C−C angles between 0° and 2°, and a deviation of the dihedral angle describing the ligand folding of 2°. RHF calculations for **2b** with the basis set [622211/4221/4111] for Zr and 6-311G* for C and H yielded deviations in Zr−C bond length between 0.06−0.02 Å and deviations of C−C−C angles between 0° and 2°.

Table 3. Listing of the Vertical Ionization Energies, $I_{v,j}$, Calculated Ionization Energies (ΔMP2), and Relative Band Intensities from He(I) and He(II) PE Spectra of 3a−c[a]

compound	band	$I_{v,j}$	assignment[a]	ΔMP2[b]	relative intensities He(I)	He(II)
3a	1	6.7	$16b_2$	6.60	1.0	1.0
	2	7.3	16a	7.83	1.0	1.0
	3	7.8	$15b_2$	8.04	1.0	1.0
	4	8.8	15a	8.87	0.8	0.9
	5	9.4	$14b_1$	*d*	0.7	0.9[e]
	6	9.6	$14b_3$	9.65	0.7	0.9[e]
3b	1	6.7	$16b_2$	6.62	0.9	0.9
	2	7.4	16a	7.39	1.0	1.0
	3	7.9	$15b_2$	7.61	1.0	1.0
	4	8.9	15a	8.65	0.9	0.7[e]
	5	9.3	$14b_1$	9.18	0.8	0.6[e]
	6	9.8	$14b_3$	9.75	0.8	0.6[e]
3c	1	6.6	$16b_2$	6.66	0.9	0.9
	2	7.3	16a	7.15	1.0	1.0
	3	7.9	$15b_2$	7.72	1.0	1.0
	4	9.0	15a	8.83	0.8	0.8[e]
	5	9.3	$14b_1$	9.44	0.7	0.9[e]
	6	9.8	$14b_3$	9.85	0.7	0.9[e]

[a] The ionization energies and orbital energies are given in eV. [b] The assignment of the bands to MOs is based on the assumption of D_2-symmetry for all three molecules. The numbering refers to the results of the HF calculations. [c] The results of the ΔMP2 calculations are based on the geometries of lowest energy. [d] No convergence could be achieved. [e] Average value.

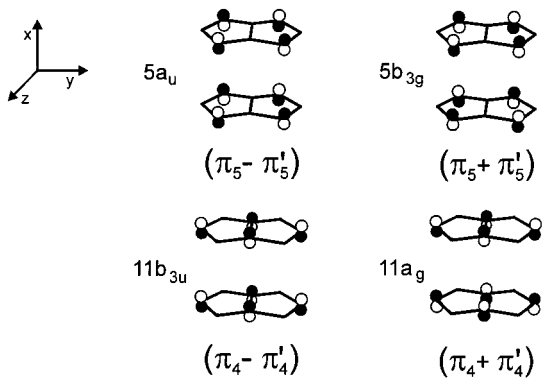

Figure 2. Schematic drawing of linear combinations arising from the ligand orbitals π_4 and π_5 assuming point group D_{2h}.

reasons of symmetry none of the metal orbitals can interact with the HOMO for either D_{2h} or D_{2d} symmetry. By reducing the symmetry to D_2, however, a mixing with metal $3d_{xy}$ AOs in a bonding fashion is possible. A Mulliken population analysis yields 5% metal character for $16b_2$ (in D_2) and 14% in the C_1 symmetry case. As a result, there is considerable stabilization. In the point group D_{2d} the HOMO transforms according to A_2 and thus again a linear combination with a metal-centered atomic orbital is prevented by symmetry. The HOMO-1 ($11b_{3u}$ in D_{2h}) can be described as the antibonding linear combination of the π_4-pentalene orbitals (Figure 2). For reasons of symmetry $11b_{3u}$ can interact with $4p_x$; however, this interaction is small due to the large energy difference between both basis orbitals. Thus a Mulliken population analysis yields an admixture of only 2.5% of the metal. By lowering the symmetry to D_2, an interaction with $3d_{yz}$ is possible. This leads to a stronger mixture of ligand and metal orbitals (9% metal character D_2, 15% C_1), and accordingly a further stabilization below orbital 16a results. In point group D_{2d} the $3d_{x^2-y^2}$ and the $3d_{xy}$ can interact with the $\pi_4-\pi_4'$ linear combination ($11b_2$). The ($\pi_5 + \pi_5'$) linear combination of the pentalene MOs transforms according to $5b_{3g}$ in point group D_{2h}. This allows a strong bonding interaction with the $3d_{yz}$ orbital of the metal (18% metal character). By reducing the symmetry the metal−ligand interaction is reduced and corresponds to a minimum at D_2 (13%) and 14% C_1. A further rotation of the two ligands leads to point group D_{2d} in which now the ligand MO transforms according to $5b_1$ and interacts with the $3d_{xy}$ metal orbital. This interaction (14%) is weaker than in D_{2h} but still stronger than in D_2 for overlap reasons. The fourth orbital from the top can be described as a linear combination of the $11a_g$ ligand orbital ($\pi_4 + \pi_4'$) with the $3d_{x^2-y^2}$ orbital (13%) of the metal center. By changing the symmetry to either D_2 or D_{2d} the metal participation is only slightly reduced (12%, D_2; 15% C_1, 12% D_{2d}), and thus a slight destabilization results. The other two MOs, $7b_{1u}$ and $6b_{2g}$, correlate with 14e. Both show a moderate metal character of 5−11% during the process of rotation of the ligands, therefore leading to only minor differences. The correlation diagram in Figure 1 suggests that the dication of **3a** should prefer D_{2d} structure. This prediction is in line with the results of DFT calculations on **3a**.[6]

Photoelectron Spectroscopic Investigations. In those cases where the validity of the Koopmans' picture[11] can be assumed and where orbital energies are dependent on conformational changes, PE spectroscopy has been used as a tool to elucidate the conformation of molecules in the gas phase.[12] Therefore we measured the He(I) PE spectra of **3a**−**c**. In addition also the He(II) PE spectra were recorded (Figure 3). To assign the PE bands to ionization events, we rely on MO calculations and we compare the band intensities of the He(I) PE spectra with those of the He(II) spectra, making use of the observation that the PE cross sections of metal d orbitals and ligand MOs differ significantly.[13] Bands associated with ionizations from MOs of strong d character are considerably enhanced in the He(II) spectra relative to those bands that originate from ligand orbitals. This is usually observed for "late" transition metal derivatives, such as in the case of the metallocenes of Cr, Mn, Fe, Co, and Ni,[14] whereas in the biscyclopentadienylmetal derivatives of group IVb the intensity differences for bands originating from the metal and the Cp ligand are rather small.[15]

The spectra are displayed in Figure 3 and the vertical ionization energies, $I_{v,j}$, are collected in Table 3. In all three He(I) spectra we recognize between 6.6 and 10 eV six bands. In the He(II) spectra the bands at higher energy (4−6) overlap stronger due to the lower resolution (ca. 180−200 cps) compared to the He(I) spectra

(11) Koopmans, T. *Physica* **1934**, *1*, 104−113.
(12) Klessinger, M.; Rademacher, P. *Angew. Chem.* **1979**, *91*, 885−896; *Angew. Chem., Int. Ed. Engl.* **1979**, *18*, 826−837. Brown, R. R.; Jorgensen, F. S. *Electron Spectroscopy: Theory, Techniques, and Applications*; Brundle, C. R., Baker, A. D., Eds.; Academic Press: London, 1984.
(13) Connor, J. A.; Derrick, L. M. R.; Hall, M. B.; Hillier, I. H.; Guest, M. F.; Higginson, B. L.; Lloyd, D. R. *Mol. Phys.* **1974**, *28*, 1193−1205.
(14) Cauletti, C.; Green, J. C.; Kelly, M. R.; Powell, P.; van Tilborg, J.; Robbins, J.; Smart, J. *J. Electron Spectrosc. Relat. Phenom.* **1980**, *19*, 327−353. Cooper, G.; Green, J. L.; Payne, M. P. *Mol. Phys.* **1988**, *63*, 1031−1051.
(15) Cauletti, C.; Clark, J. P.; Green, J. C.; Jackson, S. E.; Fragala, I. L.; Ciliberto, E.; Coleman, A. W. *J. Electron Spectrosc. Relat. Phenom.* **1980**, *18*, 61−73.

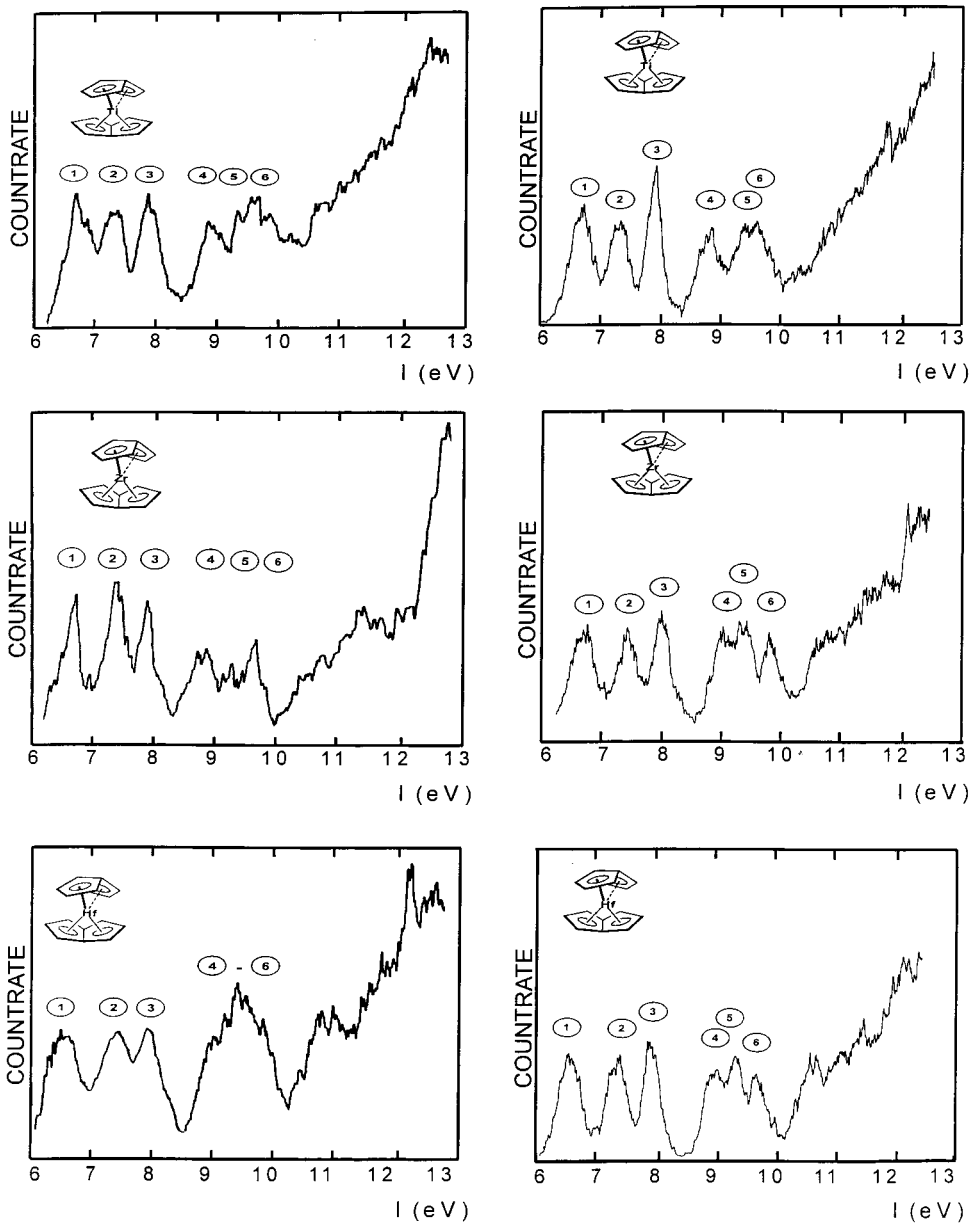

Figure 3. He(I) (right) and He(II) (left) photoelectron spectra of **3a** (top), **3b** (center), and **3c**.

(400 cps). We assign each of the six bands to a single ionization event due to the observation that the areas below the bands are very similar (see Table 3). A comparison between the intensities of the He(I) and He(II) spectra (columns 6 and 7 of Table 3) show slight variations of the intensity ratios between the first six peaks. This indicates very similar d character for the highest six MOs. In the last column of Table 4 the metal d character is listed. In the case of **3b**, the ionization events from the three highest occupied orbitals (corresponding to bands 1−3) increase by ca. 30% when comparing the He(II) spectrum with the He(I) spectrum relative to bands 4−6. This correlates well with the metal d character of the respective orbitals. The sum of the metal d character for the orbitals 1−3 is 26.7 and 20.1 for orbitals 4−6. This yields a ratio of 0.57:0.43 or 1.33:1.00. For **3b** and **3c** the calculations predict a low d character for the HOMO (ca. 4−5%). This, however, is restricted to D_2 symmetry only and not to C_1. In the latter case values similar to **3a** are obtained due to a strong mixing of metal and ligand orbitals. This result is in line with detailed calculations of Koopmans' defects for ionization processes of complexes of transition elements of groups IIIb−Vb.[16]

Our assignment of the PE bands to individual ionizations is based on the assumption that the Koopmans' picture[16] is valid. Effects of electron correlation and relaxation of orbitals can spoil the validity of Koopmans' theorem. To probe this, we have calculated the energy difference between the various ionic states and the ground state of **3a**−**c** using Møller−Plesset second-order perturbation theory (ΔMP2)[17] and the Hartree−Fock wave functions as reference functions. A comparison between the recorded ionization energies and the ΔMP2 values is very good. A comparison with the calculated orbital energies (Table 4) and the ΔMP2 energies (Table

(16) Böhm, M. C. *Inorg. Chem. Acta* **1982**, *62*, 171−182; *J. Chem. Phys.* **1983**, *78*, 7044−7064.
(17) Møller, C.; Plesset, M. S. *Phys. Rev.* **1934**, *46*, 618−622.

Table 4. Calculated Orbital Energies, ϵ_j, Composition Wave Functions, and Metal Character (%) of the Wave Functions[a]

compound	$-\epsilon_j$[b]	symmetry	wave functions	metal char. (%)[c]
3a	6.62	62a	π_5^-/yz	13.5
(C_1)	7.75	61a	π_5^+/z^2	14.0
	7.91	60a	π_4^-/yz	14.7
	6.69	59a	π_4^+/x^2-y^2	15.1
	10.46	58a	π_3^+/xz	15.8
	10.59	57a	π_3^-/yz	16.0
3b	6.71	$16b_2$	π_5^-/yz	4.2
(D_2)	7.61	16a	π_5^+/z^2	12.5
	8.03	$15b_2$	π_4^-/yz	10.0
	8.59	15a	π_4^+/x^2-y^2	12.1
	10.30	$14b_1$	π_3^+/xz	8.2
	10.85	$14b_2$	π_3^-/yz	9.8
3c	6.77	$16b_2$	π_5^-/yz	4.6
	7.62	16a	π_5^+/z^2	19.6
	8.09	$15b_2$	π_4^-/yz	7.6
	9.65	15a	π_4^+/x^2-y^2	7.4
	10.44	$14b_1$	π_3^+/xz	10.9
	10.89	$14b_2$	π_3^-/yz	10.9

[a] The orbital energies are given in eV. [b] The calculated values correspond to the geometries of lowest energies for **3a**−**c**. [c] The metal contribution to the wave function results from a Mulliken overlap population analysis.

3) confirms the validity of the Koopmans' picture since the order of the orbitals is the same.

As pointed out in the previous paragraph we expect for **3a**−**c** a symmetry close to D_2. For such a case two groups of bands (1−3 and 4−6) should be separated by a larger gap (see Figure 1). This is indeed the case. Bands 1−3 are separated by 0.5−0.7 eV, bands 4−6 by 0.2−0.6 eV, whereas both groups are separated by 1.0−1.1 eV.

Conclusion

The combination of high-level ab initio calculations and PE spectroscopy has allowed us to assign the orbital sequences of the homoleptic parent pentalene complexes **3a**−**c**. Furthermore, the studies have shown that the conformation of the ligands in the gas phase is at least reasonably close to D_2. The main driving force for this conformation can be traced back to electronic effects. The weakly antibonding character of the HOMO in D_{2h} and D_{2d} symmetry is turned into a bonding one when the symmetry is reduced. This effect is enforced by a mixing between antibonding ligand orbitals of $11b_{3u}$ and metal orbitals.

Experimental Section

The preparation of **3a**−**c** has been reported in the literature.[2b] The photoelectron spectra were recorded with a PS18 spectrometer (Perkin-Elmer) at 175 °C (**3a**) and 160 °C (**3b**,**c**). The spectrometer was equipped with a Helectros lamp capable of giving both He(I) and He(II) radiation. Where a clear separation of bands was found, relative intensities were estimated by dividing the band areas. The spectra were recorded at least twice for each complex. The count rates for He(I) were 400 cps, for He(II) 180−200 cps. The spectra were calibrated with Ar and Xe. A resolution of 20 meV was obtained for the $^2P_{3/2}$ line of Ar.

Acknowledgment. We are grateful to Tokyo Denki University, which made the stay of J.O. in Heidelberg possible. We thank the Deutsche Forschungsgemeinschaft (SFB 247), the Fonds der Chemischen Industrie, and the BASF, Ludwigshafen, for financial support. We thank Mrs. A. Reule for typing the manuscript.

Supporting Information Available: A Table of calculated Cartesian coordinates of **3a**−**c**. This material is available free of charge via the Internet at http://pubs.acs.org.

OM0102403